**Earthline Journal of Chemical Sciences**
E-ISSN: 2581-9003; CODEN: EJCSB4
Volume 12, Number 3, 2025, Pages 281-290
https://doi.org/10.34198/ejcs.12325.281290

# Effect of zinc cation on thiobarbital and a perturbed thiobarbital – A DFT treatment

**Lemi Türker**

Department of Chemistry, Middle East Technical University, Üniversiteler, Eskişehir Yolu No: 1, 06800 Çankaya/Ankara, Turkey
e-mail: lturker@gmail.com; lturker@metu.edu.tr

## Abstract

In the present study, thiobarbital and a perturbed thiobarbital which is constructed from thiobarbital by means of certain centric perturbations have been subjected to effect of zinc cation in vacuum conditions within the constraints of density functional theory at the level of B3LYP/6-31++G(d,p). Various structural and quantum chemical data have been collected and discussed, including IR and UV-VIS spectra. The effect of $Zn^{+2}$ resulted that in both of the structures considered an α-hydrogen of one of the ethyl moieties underwent a bond cleavage which seemed that it is more dramatic on thiobarbital.

## 1. Introduction

Zinc is the second most abundant trace element (after iron) essential for all living organisms. Zinc exists as a divalent cation ($Zn^{2+}$) and is not redox active under physiological conditions, which explains why zinc performs multifarious physiological roles in a variety of biological processes [1]. Zinc is an essential trace element crucial for the function of more than 300 enzymes and it is important for cellular processes like cell division and apoptosis [2].

Regulation of zinc metabolism occurs at several sites: gut absorption and endogenous secretion, urinary excretion, and the size and turnover of the rapidly (plasma, red blood cells, and liver) and slowly exchanging pools (muscle and bone). Changes in zinc metabolism with age are tissue specific. An elaborate homeostatic system of proteins regulates cellular $Zn^{2+}$ distribution and perhaps controls a hierarchy of zinc-dependent functions [3].

A critical aspect of cellular zinc metabolism is the tight control of the pico molar concentrations of free zinc ions and their fluctuations to balance folding and misfolding of proteins, supply of thousands of zinc-requiring proteins with zinc, and dual functions of zinc as either a pro-oxidant or a pro-antioxidant. Zinc/sulphur (cysteine) bonds in proteins have a key role in this control because they generate redox-active coordination environments. Metallothionein (MT) is such a redox-active zinc protein, which couples biochemically to the cellular redox state. The coordination dynamics and redox state of its zinc/thiolate clusters determine cellular zinc availability. A fraction of MT in tissues and cells contains free thiols and disulfides [3].

Zinc metabolism is adversely affected by diabetes mellitus [4]. The significance of zinc, a trace metal, in chronic liver disease has also been recently recognized [5-7].

Extensive research suggests zinc's involvement in promoting malignancy and invasion in cancer cells, despite its low tissue concentration [8].

Received: May 22, 2025; Accepted: June 30, 2025; Published: July 7, 2025

Keywords and phrases: zinc, thiobarbital isomers, interactions, vitamin D, DFT calculations.

Copyright © 2025 the Author

Studies have found that reduced blood zinc levels could predict vitamin D deficiency in adolescent girls, while zinc supplementation increased vitamin D levels in postmenopausal women. In vitro studies using human peritoneal macrophages have found that zinc induced the release of calcitriol (1,25-dihydroxycholecalciferol). Zinc also acts as a cofactor for vitamin D functions, as the transcriptional activity of vitamin D-dependent genes relies on zinc to exert pleiotropic functions, including mineral ion regulation. Vitamin D could also induce zinc transporters to regulate zinc homeostasis. Together, zinc and vitamin D in adequate concentrations help to maintain a healthy musculoskeletal system and beyond; however, deficiency in either of these nutrients can result in various disorders affecting almost all body systems [9].

Thiobarbital, also known as 5,5-diethyl-2-sulfanylidene-1,3-diazinane-4,6-dione is a barbiturate derivative that has been used in medical settings for its sedative and hypnotic properties [10,11]. Thiobarbital acts on the central nervous system (CNS) by enhancing the inhibitory effects of gamma-aminobutyric acid (GABA), which is a neurotransmitter. Thiobarbital acts on the central nervous system and this action results in sedative, hypnotic, and anticonvulsant effects. Thiobarbital has an antithyroid effect [12,13].

## 2. Method of Calculations

In the present study, all the initial optimizations of the structures leading to energy minima have been achieved first by using MM2 method which is then followed by semi empirical PM3 self consistent fields molecular orbital method [14-16]. Afterwards, the structure optimizations have been achieved within the framework of Hartree-Fock and finally by using density functional theory (DFT) at the levels of B3LYP/6-31++G(d,p) [17,18]. Note that the exchange term of B3LYP consists of hybrid Hartree-Fock and local spin density (LSD) exchange functions with Becke's gradient correlation to LSD exchange [19]. The correlation term of B3LYP consists of the Vosko, Wilk, Nusair (VWN3) local correlation functional [20] and Lee, Yang, Parr (LYP) correlation correction functional [21]. In the present study, the normal mode analysis for each structure yielded no imaginary frequencies for the $3N–6$ vibrational degrees of freedom, where $N$ is the number of atoms in the system. This search has indicated that the structure of each molecule considered corresponds to at least a local minimum on the potential energy surface. Furthermore, all the bond lengths have been thoroughly searched in order to find out whether any bond cleavage occurred or not during the geometry optimization process. All these computations were performed by using SPARTAN 06 program [22].

## 3. Results and Discussion

In the present study, effect of $Zn^{+2}$ on thiobarbital and one of its structural isomer, constructed by mutual sulphur/oxygen replacements (centric perturbations engender perturbed thiobarbital) have been investigated within the realm of density functional theory (DFT). The organic specie and the zinc cation altogether constitute a composite system which is named as $I+Zn^{+2}$ or $II+Zn^{+2}$ depending on the organic part, thiobarbital (I) or the perturbed thiobarbital (II). The ground state electronic configuration of zinc atom is $1s^2 2s^2 2p^6 3s^2 3p^6 4s^2$. Figure 1 stands for the optimized structures of the composite systems considered. The figure also displays the direction of the dipole moment vectors for the composite systems.

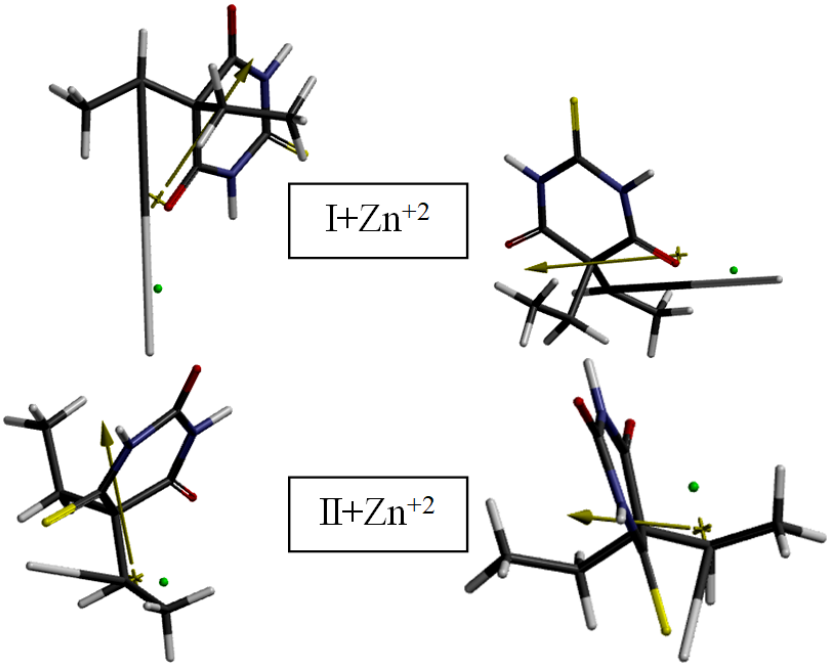


**Figure 1.** Optimized structures of the composites of thiobarbital isomers considered (different views).

As seen in the figure, both of the composites undergo some great structural changes such that in each case, one of α-C-H bonds of an ethyl substituent exhibits striking elongation, which stands for bond cleavage. The elongations for I+$Zn^{+2}$ and II+$Zn^{+2}$ systems are 6.237 Å and 2.713 Å, respectively (see Figure 2). After the optimization process the data reveal that the charge of zinc cation is no longer +2 but decreased to 1.068 and 1.374 esu, (see Figure 3) respectively for composites I+$Zn^{+2}$ and II+$Zn^{+2}$ (The natural charges are 1.249 and 1.412, respectively). Thus, the zinc cation in each case accepts some electron population from the organic partner, (acting as an oxidizer cation) being itself reduced. All these effective changes also accompanied by some other (minor) bond length and bond angle variations.

Figure 2 shows the calculated bond lengths/distances (Å) of the composites whereas the electrostatic potential (ESP) charges on atoms of the composites considered are depicted in Figure 3. Note that the ESP charges are obtained by the program based on a numerical method that generates charges that reproduce the electrostatic potential field from the entire wavefunction [22].

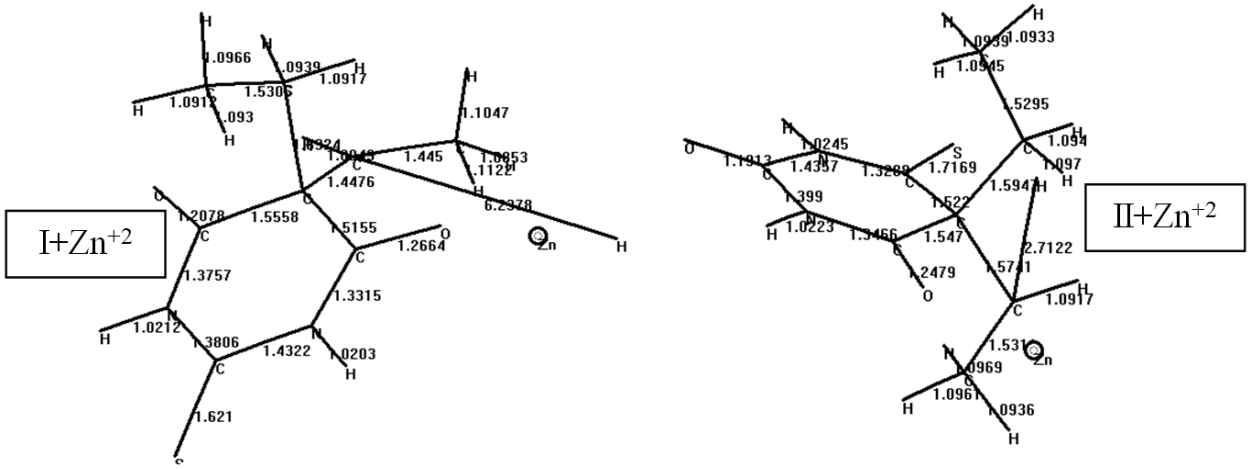


**Figure 2.** The calculated bond lengths/distances (Å) of the zinc composites of isomeric thiobarbital species considered.

Figure 3 displays the ESP charges on atoms of the composites considered. Note that more positive charge resides on the zinc atom in the case of II+$Zn^{+2}$. Keep in mind that prior to decomposition by the effect of zinc cation, structure II is the perturbed thiobarbital.

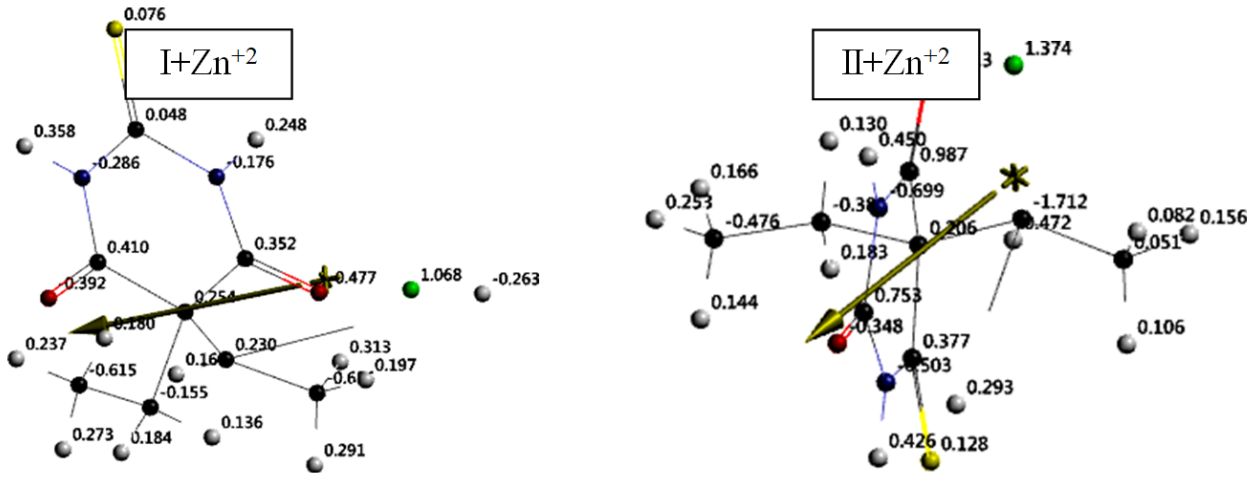


**Figure 3.** The ESP charges on atoms of the composites considered.

Figure 4 shows the calculated IR spectra of the composites considered. In IR spectrum of I+$Zn^{+2}$, the peaks at 3525 $cm^{-1}$ and 3520 $cm^{-1}$ stand for symmetrical and unsymmetrical N-H stretchings, respectively. They somehow appear as overlapped. Various C-H stretchings happen in between 3229-2937 $cm^{-1}$. The peak at 1822 $cm^{-1}$ is for one of the carbonyl (amide) stretching accompanied by ring breath. The sharpest peak stands for the other carbonyl peak and appears at 1662 $cm^{-1}$. The peak at 1539 $cm^{-1}$ is due to overlap of C=S stretching and adjacent N-H bendings.

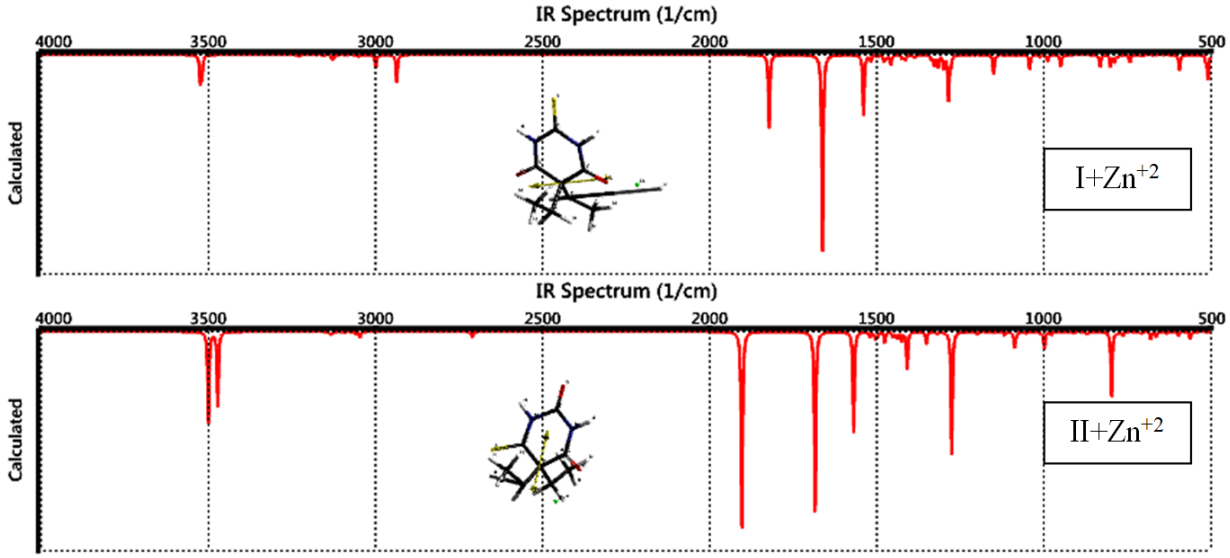


**Figure 4.** The calculated IR spectrums of the composites considered.

As for the spectrum of II+$Zn^{+2}$, the peak at 3500 $cm^{-1}$ is the N-H stretch for the imide moiety (between two C=O groups). Whereas the N-H stretch for the imide (between C=S and C=O moieties) occurs at 3422 $cm^{-1}$. The C=O moieties stretch at 1903 $cm^{-1}$ and 1684 $cm^{-1}$. The peaks at 1569 $cm^{-1}$ and 1275 $cm^{-1}$ are N-H bendings.

Table 1 shows some calculated properties of the composite species considered. All the data in Table 1 are greater for I+$Zn^{+2}$ compared to II+$Zn^{+2}$.

**Table 1.** Some calculated properties of the composite species considered.

| Composite | Dipole | Polarizability | Area (Å²) | Volume (Å³) |
|---|---|---|---|---|
| $I+Zn^{+2}$ | 7.70 | 57.17 | 233.82 | 200.51 |
| $II+Zn^{+2}$ | 5.93 | 56.37 | 220.25 | 197.02 |

Dipole moments in debye units. Polarizabilities in $10^{-30}$ $m^3$ units.

Figure 5 shows the exposed area of atoms in the composites considered. Note that the exposed surface areas of atoms are highly environment dependent [23]. They differ for the same type of atoms. For instance the doubly bounded sulphur atoms in the composites considered are quite different.

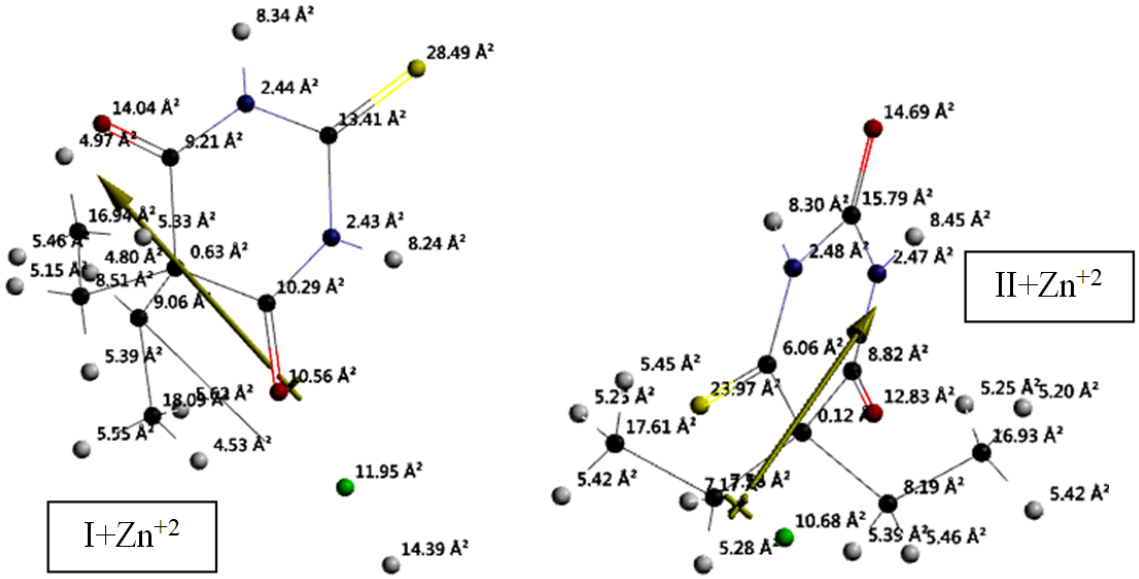


**Figure 5.** Exposed area of atoms in the composites considered.

Figure 6 shows the local ionization maps of the composites considered. Conventionally red/reddish regions (if any exists) on the density surface indicate areas from which electron removal is relatively easy, meaning that they are subject to electrophilic attack. It is worth remembering that the local ionization potential map is a graph of the value of the local ionization potential on an isodensity surface corresponding to a van der Waals surface.

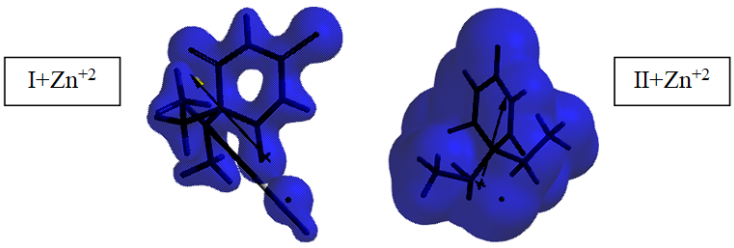


**Figure 6.** The local ionization maps of the composites considered.

Figure 7 shows the LUMO maps of the composites considered. A LUMO map displays the absolute value of the LUMO on the electron density surface. The blue color (if any exists) stands for the maximum value of the LUMO and the red colored region, associates with the minimum value. Note that the LUMO and NEXTLUMO are the major orbitals directing the molecule towards of the attack of nucleophiles [22]. Positions where the greatest LUMO coefficient exists is the most vulnerable site in nucleophilic reactions.

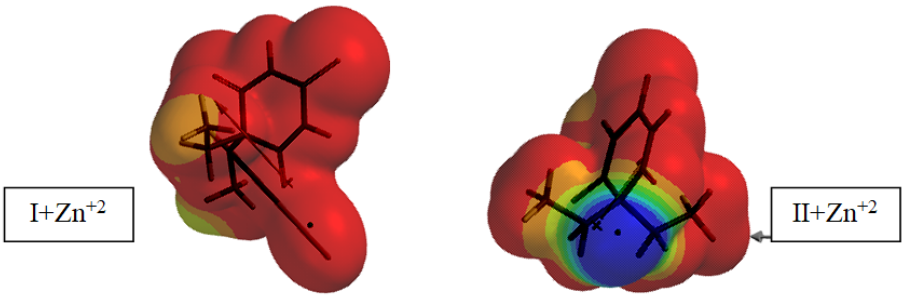


**Figure 7.** The LUMO maps of the composites considered.

Figure 8 shows the bond density maps of the zinc$^{+2}$ composites of isomeric thiobarbital species considered. In the case of I+Zn$^{+2}$, oxygen atom of carbonyl group seems to donate some electron population to Zn$^{+2}$ meanwhile α-C-H bond elongates appreciably. Whereas in the case of II+Zn$^{+2}$, it seems the zinc cation is in interaction with α-carbon of one of the ethyl groups causing the elongation of the attached C-H bond.

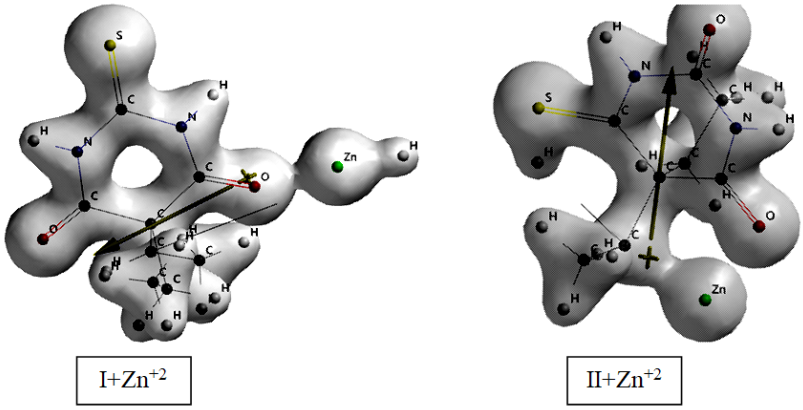


**Figure 8.** The bond density maps of the composites considered.

Figure 9 shows some of the orbital energy levels of the composites considered. The effect of zinc cation on the orbital energies is more dramatic in the case of II+Zn$^{+2}$, especially on the frontier molecular orbitals.

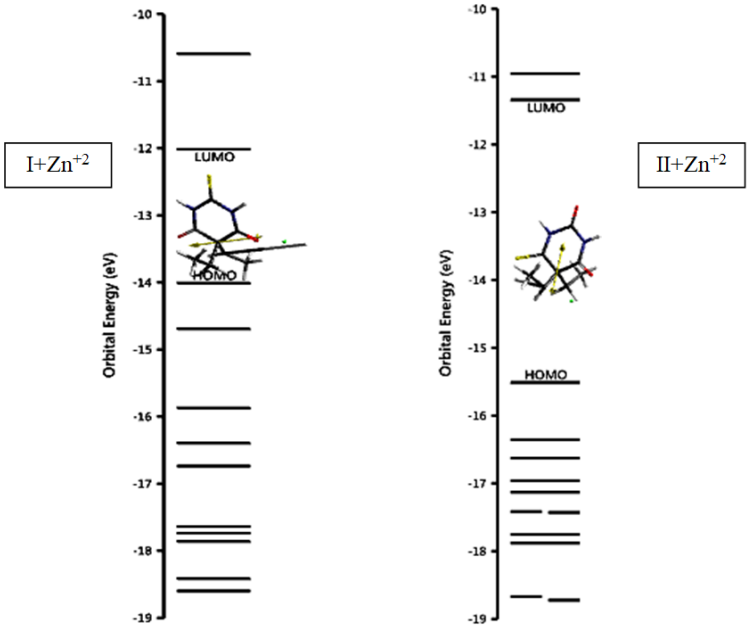


**Figure 9.** Some of the orbital energy levels of the composites of considered.

Table 2 shows the HOMO, LUMO energies and the interfrontier molecular orbital energy gap, Δε, values ($\Delta\varepsilon = \varepsilon_{LUMO}-\varepsilon_{HOMO}$) of the composites considered.

**Table 2.** The HOMO, LUMO energies and Δε values of the composites considered.

| Composite | HOMO | LUMO | Δε |
|---|---|---|---|
| $I+Zn^{+2}$ | -1351.51 | -1159.21 | 192.3 |
| $II+Zn^{+2}$ | -1496.42 | -1094.27 | 402.15 |

Energies in kJ/mol.

The algebraic orders of the HOMO and LUMO energies are $II+Zn^{+2} < I+Zn^{+2}$ and $I+Zn^{+2} < II+Zn^{+2}$, respectively. Consequently, the order of Δε values becomes $II+Zn^{+2} > I+Zn^{+2}$. All the geometrical and electronic factors operative in these decomposed composites should be responsible for that.

Figure 10 shows the HOMO and LUMO as well as the HOMO-1 and LUMO+1 patterns of the composites species considered.

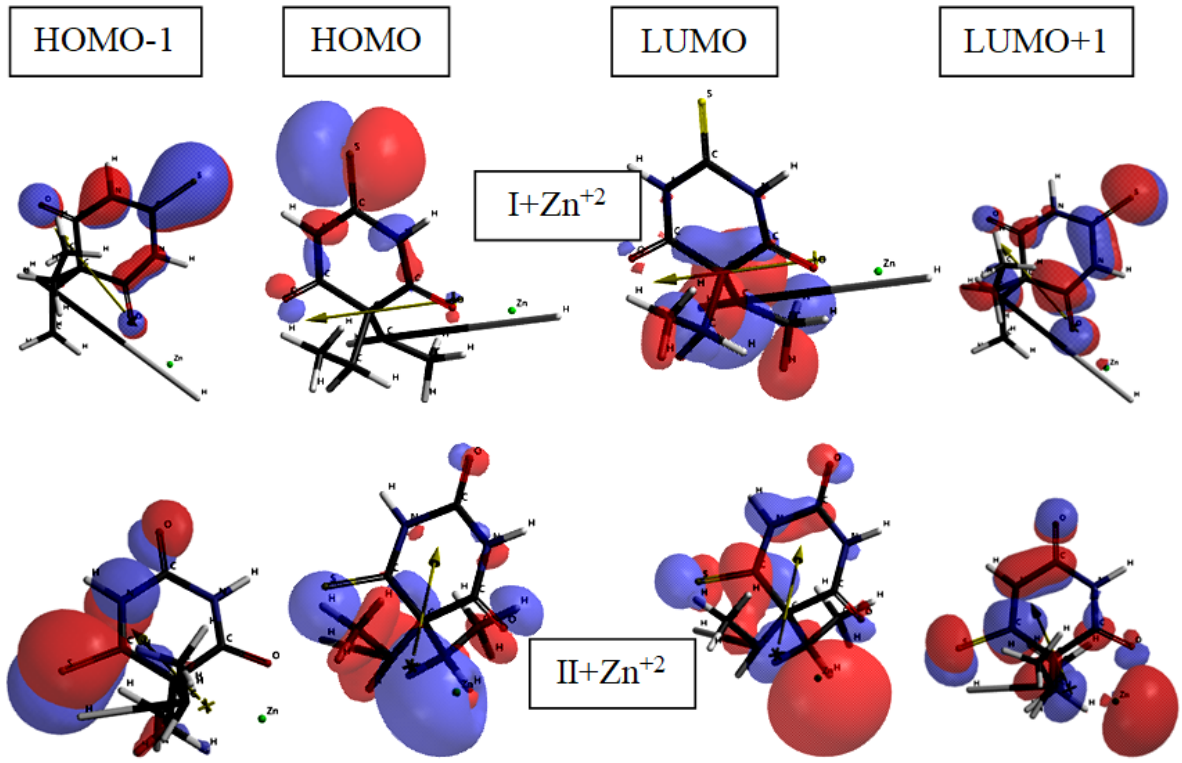


**Figure 10.** The HOMO, LUMO, NEXTHOMO and NEXTLUMO patterns of the composites species considered.

Figure 11 displays the bond density-HOMO (absolute value) maps. Whereas Figure 12 shows the ionization maps of the composites considered. Ionization potential map indicates the ease or difficulty of electron removal.

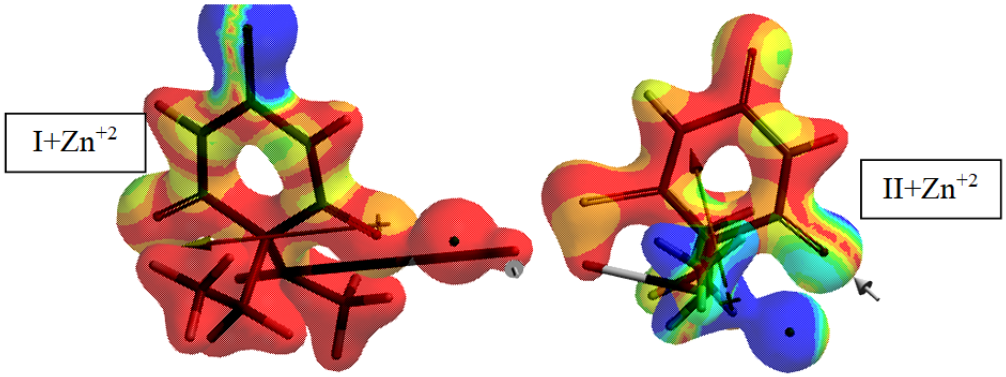


**Figure 11.** Bond density, HOMO maps.

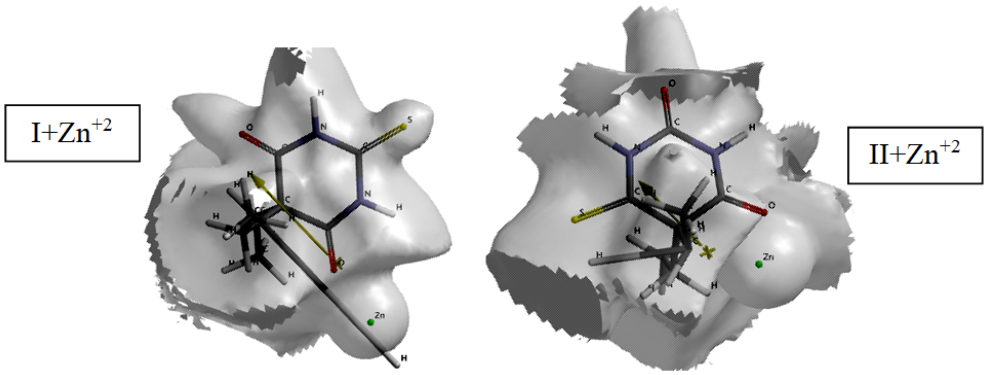


**Figure 12.** The ionization map of the composites considered.

Figure 13 displays the calculated UV-VIS spectra (time dependent DFT) of the composites considered. In spectrum of $I+Zn^{+2}$ absorption peaks are at 317, 423, and 604 nm. Such a large span of absorption implies that quite effective extended conjugation exists in the composite system. Whereas the spectrum of $II+Zn^{+2}$ does not have so distinct peaks but has a huge shoulder. Altogether the absorption spreads to 200-450 nm. The broad and overlapped peaks are at 299.60 and 347.27 nm. Since the interfrontier molecular orbital energy gap value for the $II+Zn^{+2}$ is greater, the excitation requires more energy; therefore its spectrum is confined to UV region almost completely.

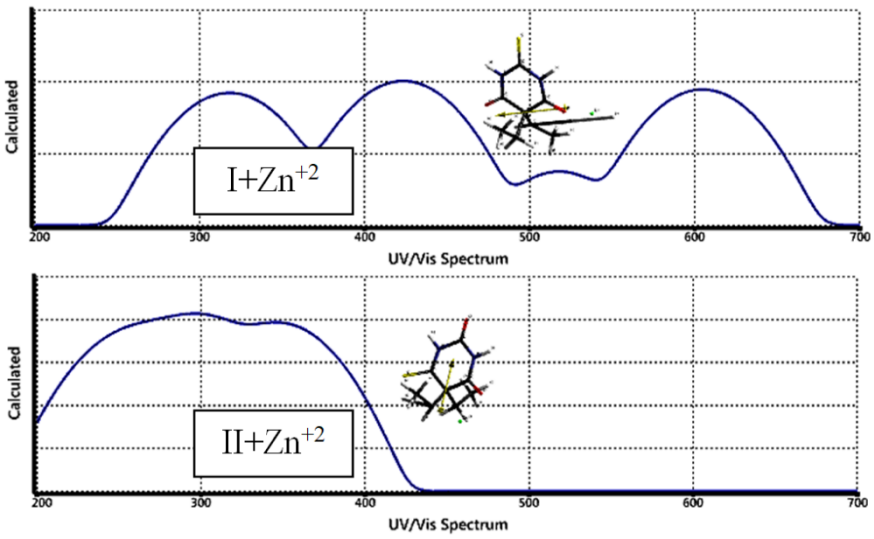


**Figure 13.** UV-VIS spectrums of the composite species considered.

## 4. Conclusion

The present computational DFT study, on thiobarbital and one of its structural isomers reveals that zinc cation affects those structures causing the C-H bond cleavage of one of the ethyl moieties present. The result of bond rupture dictates various properties of these systems. However, the calculations are true for vacuum conditions as well as the restrictions of density functional approach. It is a matter of question whether thiobarbital or similar type compounds may lead to zinc deficiency although in the living organisms zinc is usually in the chelated form by various organic or inorganic nucleophiles, thus the concentration of free zinc cation is under the control of various multiple equilibria. On the other hand, whether the zinc cation adversely diminishes the therapeutic value of thiobarbital is another point to be investigated. However further theoretical research in aqueous media or some clinical surveys may put more light on to the subject.

## References

[1] Kambe, T., Tsuji, T., Hashimoto, A., & Itsumura, N. (2015). The physiological, biochemical, and molecularroles of zinc transporters in zinc homeostasis and metabolism. *Physiol. Rev., 95*, 749-784. https://doi.org/10.1152/physrev.00035.2104

[2] Jansen, J., Karges, W., & Rink, L. (2009). Zinc and diabetes - clinical links and molecular mechanisms. *Journal of Nutritional Biochemistry, 20,* 399-417. https://doi.org/10.1016/j.jnutbio.2009.01.009

[3] Maret, W. (2008). Metallothionein redox biology in the cytoprotective and cytotoxic functions of zinc. *Experimental Gerontology*, *43*(5), 363-369. https://doi.org/10.1016/j.exger.2007.11.005

[4] Ranasinghe, P., Pigera, S., Galappatthy, P., Katulanda, P., & Constantine, G.R. (2015). Zinc and diabetes mellitus: understanding molecular mechanisms and clinical implications. *DARU Journal of Pharmaceutical Sciences, 23*(44). https://doi.org/10.1186/s40199-015-0127-4

[5] Stamoulis, I., Kouraklis, G., & Theocharis, S. (2007). Zinc and the liver: An active interaction. *Dig, Dis. Sci., 52*, 1595-1612. https://doi.org/10.1007/s10620-006-9462-0

[5] Grungreiff, K., Reinhold, D., Wedemeyer, H. (2016). The role of zinc in liver cirrhosis. *Ann. Hepatol.*, *15*, 7-16. https://doi.org/10.5604/16652681.1184191

[7] Katayama, K., Kawaguchi ,T., Shiraishi, K., Ito, T., Suzuki, K., Koreeda, C., Ohtake, T., Iwasa, M., Tokumoto, Y., Endo, R., Kawamura, N., Shiraki, M., Hanai, T., Habu, D., Tsuruta, S., Sakai, H., Miwa, Y., Kawada, N., Kato, A., Takei, Y., Mine, T., Kohgo, Y., Seki, T., Sata, M., Ito, Y., Fukui , K., Nishiguchi, S., Moriwaki, H., & Suzuki, K. (2018). The prevalence and implication of zinc deficiency in patients with chronic liver disease. *J. Clin. Med. Res.*, *10*, 437-444. https://doi.org/10.14740/jocmr3374w.Epub

[8] Cellular zinc metabolism and zinc signaling: from biological functions to diseases and therapeutic targets. Chen, B., Yu, P., Cha, W.N., Xie, F., Zhang, Y. Li, L. , Leung, K.T., Lo, K.W., Yu, J., Tse, G.M.K., Kang, W., & To,K.F. (2024). *Signal Transduction and Targeted Therapy, 9*(1), 6. https://doi.org/10.1038/s41392-023-01679-y

[9] Amos, A., & Razzaque, M.S. (2022). Zinc and its role in vitamin D function. *Current Research in Physiology*, *5*, 203-207. https://doi.org/10.1016/j.crphys.2022.04.001

[10] Fischer, E., & Dilthey, A. (1904). Ueber C-Dialkylbarbitursäuren und über die Ureïde der Dialkylessigsäuren. *Justus Liebigs Annalen der Chemie*, *335*(3), 334-368. https://doi.org/10.1002/jlac.19043350303

[11] Carrington, H.C. (1965). The action of phosphorus pentasulphide on barbituric acids. *Journal of the Chemical Society* (Resumed), 1 to 7601. https://doi.org/10.1039/JR9440000124

[12] Bartels, E.C. (1945). Use of thiobarbital in the treatment of hyperthyroidism. *JAMA, 129*(14), 932-935. https://doi.org/10.1001/jama.1945.02860480012003

[13] Mansberger, A.R., Jr. (1988). One hundred years of surgical management of hyperthyroidism. *Ann. Surg., 207*(6), 724-9. https://doi.org/10.1097/00000658-198806000

[14] Stewart, J.J.P. (1989). Optimization of parameters for semi-empirical methods I. *J. Comput. Chem.*, *10*, 209-220. https://doi.org/10.1002/jcc.540100208

[15] Stewart, J.J.P. (1989). Optimization of parameters for semi-empirical methods II. *J. Comput. Chem., 10*, 221-264. https://doi.org/10.1002/jcc.540100209

[16] Leach, A.R. (1997). *Molecular modeling*. Essex: Longman.

[17] Kohn, W., & Sham, L.J. (1965). Self-consistent equations including exchange and correlation effects. *Phys. Rev.*, *140*, 1133-1138. https://doi.org/10.1103/PhysRev.140.A1133

[18] Parr, R.G., & Yang, W. (1989). *Density functional theory of atoms and molecules*. London: Oxford University Press.

[19] Becke, A.D. (1988). Density-functional exchange-energy approximation with correct asymptotic behavior. *Phys. Rev. A*, *38*, 3098-3100. https://doi.org/10.1103/PhysRevA.38.3098

[20] Vosko, S.H., Wilk, L., & Nusair, M. (1980). Accurate spin-dependent electron liquid correlation energies for local spin density calculations: a critical analysis. *Can. J. Phys*., *58*, 1200-1211. https://doi.org/10.1139/p80-159

[21] Lee, C., Yang, W., & Parr, R.G. (1988). Development of the Colle-Salvetti correlation energy formula into a functional of the electron density. *Phys. Rev. B*, *37*, 785-789. https://doi.org/10.1103/PhysRevB.37.785

[22] SPARTAN 06 (2006). Wavefunction Inc. Irvine CA, USA.

[23] Richmond, T.J. (1984). Solvent accessible surface area and excluded volume in proteins: Analytical equations for overlapping spheres and implications for the hydrophobic effect. *Journal of Molecular Biology*, *178*(1), 63-89. https://doi.org/10.1016/0022-2836(84)90231-6

This is an open access article distributed under the terms of the Creative Commons Attribution License (http://creativecommons.org/licenses/by/4.0/), which permits unrestricted, use, distribution and reproduction in any medium, or format for any purpose, even commercially provided the work is properly cited.